Aktuelle Forschung in der Biomechanik

Martin Mössner

martin.moessner@uibk.ac.at
2. Mai 2024

Das Knie

Knie: Bücher

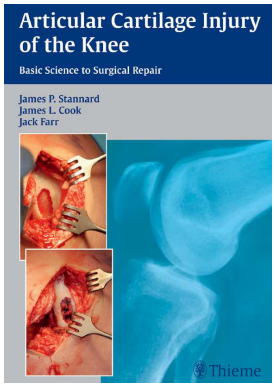

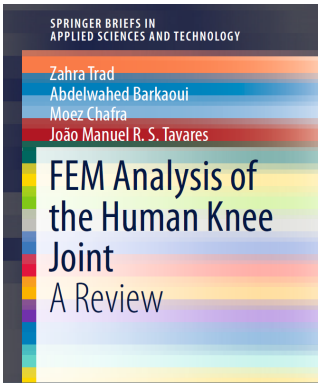

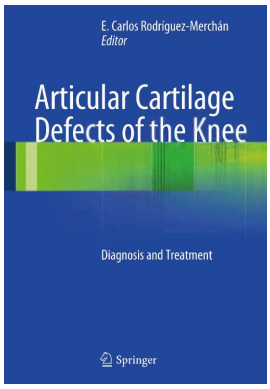

Statische Kräfte im Knie: Gewichtheben

m = 320 kg	Gewicht + Körper
L = 0.4 m	Oberschenkel
d = 0.05 m	Knieradius
F_Q = ?	Quadrizepskraft

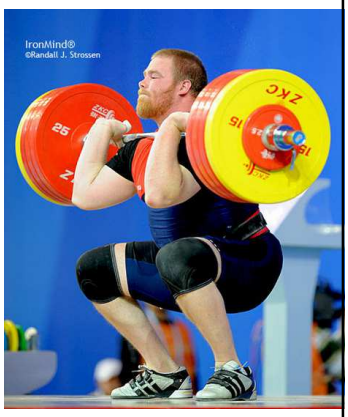

Momentgleichgewicht um Knieachse

$M_{Knie} = m\,g \cdot L/2 = 2 \cdot F_Q \cdot d$

$M_{Knie} = 628$ Nm

$F_Q = 6278$ N

Statische Kräfte im Knie

F_Q Quadrizepskraft
F_{PL} Patellasehne
F_R Kompressionskraft Patella

Kräftegleichgewicht:

$F_R \cdot \cos\alpha - F_Q \cdot \sin\theta - F_{PL} \cdot \sin\beta = 0$
$F_R \cdot \sin\alpha + F_Q \cdot \cos\theta - F_{PL} \cdot \cos\beta = 0$

Momentgleichgewicht

$F_Q \cdot m_Q = F_{PL} \cdot m_{PL}$

α, β, m_Q, m_Q siehe Nisel (1985)

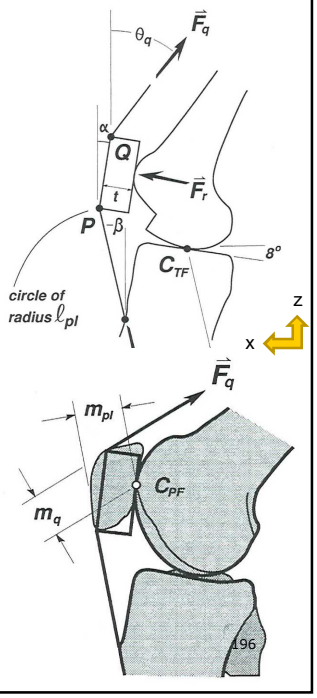

Statische Kräfte im Knie: Gewichtheben

θ=90°, β=2°, α=36°
m_Q=15 mm, m_{PL}=20 mm

F_Q = 6278 N

$0.8090\ F_R - 6278 - 0.0349\ F_{PL}=0$
$0.5878\ F_R - 0.9994\ F_{PL}=0$

F_{PL}=4683 N
F_R =7962 N

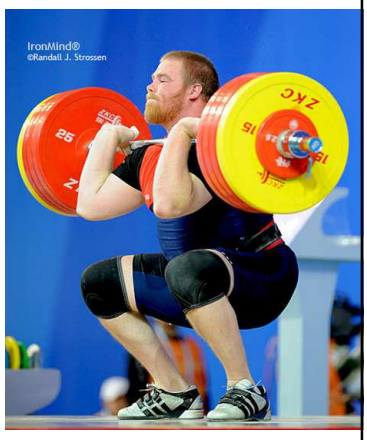

Richtung und Hebelarm der Kräfte im Knie

Herzog & Read (1993) Lines of Action and Moment Arms of the Major Force-Carying Structures Crossing the Human Knee Joint

Untersuchung an 5 Leichen im Alter von 80 J

Wirkungsrichtung der Kraft und
Hebelarm bzgl. tatsächlicher Drehachse im Knie

Patellasehne
Bizeps Femoris, Semitendinosus, Semimembranosus
Anterior, Posterior, Lateral und Medial Cruciate

Patellasehne

Kraftrichtung

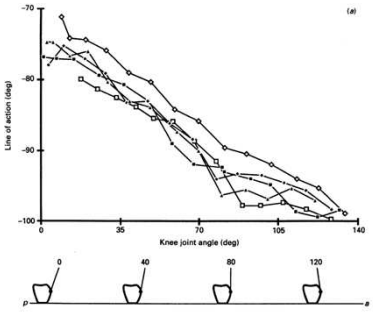

Momentarm

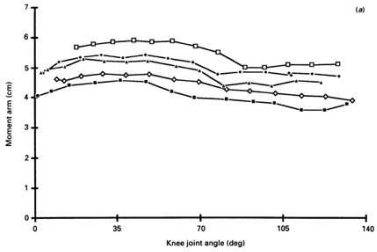

Herzog & Read 1993

$\beta = -74.4-0.057\cdot\theta-0.05\cdot\theta^2$ (°)
(β = -90° = senkrecht)

$d = 4.71+0.04\cdot\theta-0.01\cdot\theta^2$ (cm)
(bzgl. Drehachse)

Kniebänder

Richtung Vorderes Kreuzband

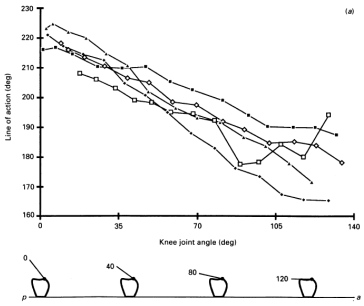

$\beta = 227\text{-}0.448 \cdot \theta$ (°)

Herzog & Read 1993

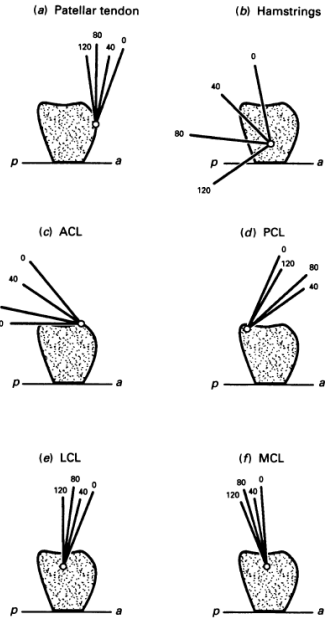

ACL: Festigkeit

Woo et al. 1990:

Age (y)	Stiffness (N/mm)	Failure Load (N)
22-35	242±28	2160±157
40-50	220±24	1503±83
60-97	180±25	658±129

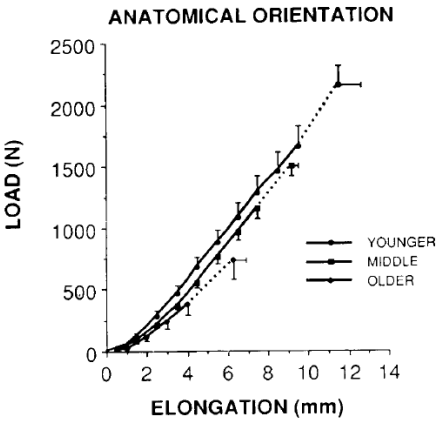

Stapleton et al. 1998:

Failure: men 2250 N, women: 1800 N

Paschos et al. 2010:

Stiffness 57.2±23.5 N/mm, Failure 400±248 N
(10 cadaver knees, 73.6±15.8 y)

Girgis et al. 1975 (24 Knie):

ACL: Länge 38.2 mm, Dicke 11.1 mm

Mündermann et al. (2014) Total knee replacement

Mündermann et al. (2014)

In Vivo Knee Loading Characteristics during Activities of Daily Living as Measured by an Instrumented Total Knee Replacement

ABSTRACT: We examined the relationship between activity, peak load, medial to lateral load distribution, and flexion angle at peak load for activities of daily living. An instrumented knee prosthesis was used to measure knee joint force simultaneously with motion capture during walking, chair sit to stand and stand to sit, stair ascending and descending, squatting from a standing position, and golf swings. The maximum total compressive load at the knee was highest during stair ascending and descending and lowest during rising from a chair. Maximum total compressive load occurred at substantially different flexion angles ranging from 8.5° during walking to 91.8° during squatting. For all activities, total compressive load exceeded 2 times body weight, and for most activities 2.5 times body weight. Most activities placed a greater load on the medial compartment than the lateral compartment. Activities were grouped into three categories: high cycle loading (walk), high load (stair ascent, descent, and golf), and high flexion angle (chair sit to stand/stand to sit, and squat). The results demonstrate that the forces and motion sustained by the knee are highly activity-dependent and that the unique loading characteristics for specific activities should be considered for the design of functional and robust total knee replacements, as well as for rehabilitation programs for patients with knee osteoarthritis or following total knee arthroplasty. © 2008 Orthopaedic Research Society. Published by Wiley Periodicals, Inc. J Orthop Res 26:1167–1172, 2008

Mündermann et al. (2014) Total knee replacement

Instrumentalisierte Knie-Prothese wurde implantiert

Testperson: 81-jähriger Mann, 1.70 m, 64.5 kg

Prothese 1.5 Jahre implantiert bevor Messungen durchgeführt.

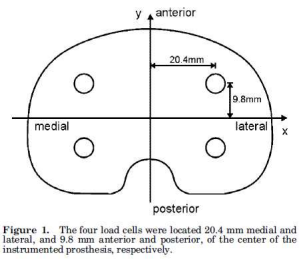

Figure 1. The four load cells were located 20.4 mm medial and lateral, and 9.8 mm anterior and posterior, of the center of the instrumented prosthesis, respectively.

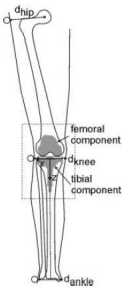

Figure 2. Anterior view of the right limb showing skin marker and implant locations relative to the femur and tibia. The information in the dotted box was taken from a postoperative radiograph.

Mündermann et al. (2014) Total knee replacement

Bestimmung der Kinematik mit 7 Kameras mit 120 fps
(MCU240, Qualisys Medical AB, Gothenburg, SE)

Bodenreaktionskräfte mit Kraftmessplatte, 120 Hz
(Bertec, Columbus, OH, US)

Das instrumentalisierte Knie zeichnete Kraftwerte an 4 Stellen der Tibia mit 70 Hz auf. Summe der Kraftsensoren im Knie wurde durch Gewichtskraft dividiert → Angabe in BW

Mündermann et al. (2014) Total knee replacement

Bei geringer Belastung (1 BW)
sind große Bereiche des Kniewinkels möglich.

Steigt die Belastung, so reduziert sich
der Bereich der möglichen Kniewinkel.

Der Kniewinkel mit max. Belastung
ist für jede Tätigkeit ein anderer!
→ wichtig für Design des Implantats!

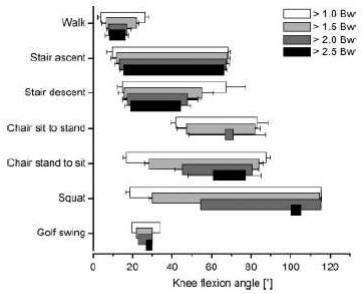

Figure 4. Range (±SD) of flexion angles for the seven activities of daily living when the total compressive load exceeds a threshold of 1.0, 1.5, 2.0, and 2.5 times BW, respectively. All reported values occurred during ground contact.

Mündermann et al. (2014) Total knee replacement

Viele Bewegungen zeigen während des Bodenkontakts hauptsächlich kleine Belastungen des Knies (< 2 BW).
Zeit/Prozentsatz mit hoher Belastung gering.

Im Gegensatz:
Stiegen steigen belastet das Knie zu einem großen Teil mit hohen Werten

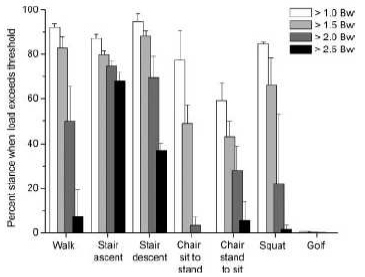

Figure 5. Percent of stance (±SD) when total compressive load exceeds a threshold of 1.0, 1.5, 2.0, and 2.5 times BW, respectively, for each of the seven activities of daily living. Percent stance was calculated as total duration of values above the threshold relative to the duration of stance.

Silverman et al. (2014) Knee joint forces for amputees

Silverman et al. (2014) 3D knee joint contact forces during walking in unilateral transtibia amputees

A B S T R A C T

Unilateral, below-knee amputees have altered gait mechanics, which can significantly affect their mobility. Below-knee amputees lose the functional use of the ankle muscles, which are critical during walking to provide body support, forward propulsion, leg-swing initiation and mediolateral balance. Thus, either muscles must compensate or the prosthesis must provide the functional tasks normally provided by the ankle muscles. Three-dimensional (3D) forward dynamics simulations of amputee and non-amputee walking were generated to identify muscle and prosthesis contributions to amputee walking mechanics, including the subtasks of body support, forward propulsion, leg-swing initiation and mediolateral balance. Results showed that the prosthesis provided body support in the absence of the ankle muscles. The prosthesis contributed to braking from early to mid-stance and propulsion in late stance. The prosthesis also functioned like the uniarticular soleus muscle by transferring energy from the residual leg to the trunk to provide trunk propulsion. The residual-leg vasti and rectus femoris reduced their contributions to braking in early stance, which mitigated braking from the prosthesis during this period. The prosthesis did not replace the function of the gastrocnemius, which normally generates energy to the leg to initiate swing. As a result, lower overall energy was delivered to the residual leg. The prosthesis also acted to accelerate the body laterally in the absence of the ankle muscles. These results provide further insight into muscle and prosthesis function in below-knee amputee walking and can help guide rehabilitation methods and device designs to improve amputee mobility.

Silverman et al. (2014) Knee joint forces for amputees

Simulationsstudie ähnlich Liu et al. (2008) fürs Gehen bzw. Hamner et al. (2010) fürs Laufen.

Prothesenträger:
Ein Fuß ist passives Segment ohne Muskulatur

Vergleichsprobanden:
Standardmodell von Hamner

Silverman et al. (2014) Knee joint forces for amputees

Probanden:

14 Prothesenträger: 45.1±9.1 Jahre, 90.5±18.6 kg, 1.75±0.10 m
Zeit seit Amputation: 5.6±2.9 Jahre,
Energy Storage and Return Prothese (ESAR) n=9,
Solid Ankle Cushioned Heel (SACH) n=5,
Ursache: 11 traumatisch, 3 vaskulär

10 Nichtamputierte: 34.1±13.0 Jahre, 70.9±13.6 kg, 1.76±0.11 m

Silverman et al. (2014) Knee joint for amputees

Personen mit Knieprothese benötigen deutlich mehr Kraft während der Standphase beim Gehen

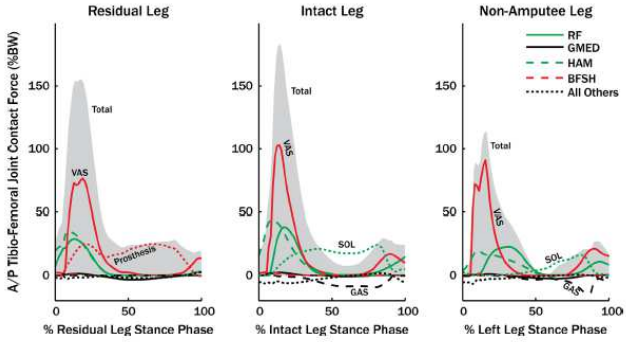

Fig. 1. Ipsilateral leg muscle group contributions to the anterior/posterior (A/P) tibio-femoral joint contact force over the stance phase. Forces are acting on the tibia and anterior is defined as positive.

DeMers et al. (2014) Changes in tibiofemoral forces due to variations in muscle activity during walking

Beim Gehen treten zum Teil hohe Belastungen zwischen Tibia und Femur auf. Insbesondere während des Ballenabdrucks in der Standfase.

Risiko der Abnutzung der Knorpel und Menisci im Knie.

Frage: Wie ändert sich die Belastung im Knie bei unterschiedlicher Muskelkoordination, d.h. unterschiedliche Aktivierung der beteiligten Muskel? Nebenbedingung: Gleiche Bewegung!

DeMers et al. (2014) Changes in tibiofemoral forces due to variations in muscle activity during walking

Gluteus Medius,
Gastrocnemius und
Rectus Femoris
haben einen gravierenden
Einfluss am Ende der
Standfase

Geringe Einflüsse beim
Fersenaufsatz

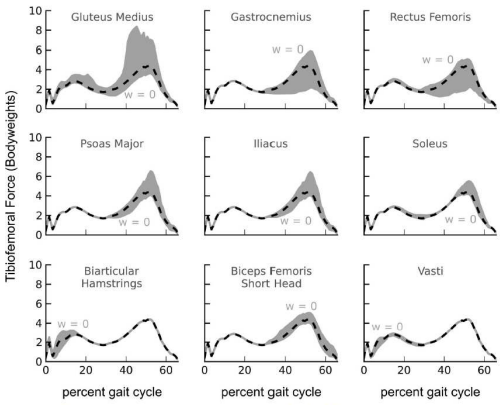

Figure 3. The effect of varying activation of individual muscles on predicted tibiofemoral forces shown for the most influential muscles. The shaded area represents the range of predicted tibiofemoral forces due to varying the activation of each muscle. For each muscle, the boundary indicated by $w = 0$ corresponded to the optimization for which the muscle activity weight of that muscle was set to zero in the objective function. This objective function permitted the muscle to activate without penalty. The model predictions that minimize uniformly-weighted muscle activations squared (dashed black lines) are shown.

Hicks et al. (2007) The effect of excessive torsion on the capacity of muscles to extend the hip and the knee in single limb stance

OpenSim Model fürs Gehen
mit 92 Muskeln

Verformung der Tibia
Durch externe Trosion des
distalen Endes (geometrische Verdillung)

Bestimmung der notwendigen
Muskelkräfte beim Gehen in
Abhängigkeit des Torsionswinkels

Anwendung: Crouch Gait, Cerebral Palsy

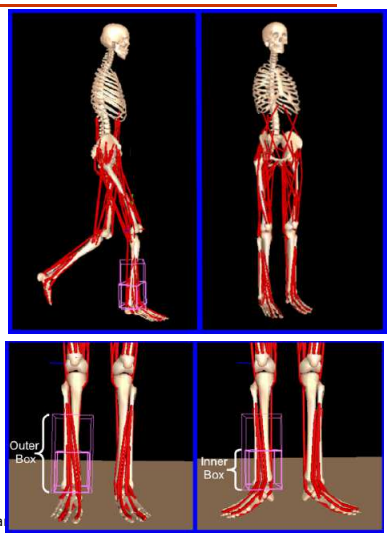

Hicks et al. (2007) The effect of excessive torsion on the capacity of muscles to extend the hip and the knee in single limb stance

Kapazität der Muskel zur Hüft- und Knieextension in Abhängigkeit der Torsion der Tibia. (A) Hüfte (B) Knie

Soleus und Gluteus können deutlich weniger zur Extension beitragen … und damit zum aufrechten Gang!

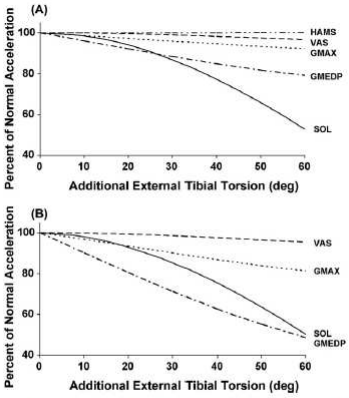

Fig. 5. The effect of excess external torsion on the average capacity of muscles to extend the hip (A) and knee (B) during single-limb stance. The accelerations per unit force are given as a percent of the values for the normal or undeformed model.

Milinkovicet al. (2023) The "Bankart knee": high-grade impression fractures of the posterolateral tibial plateau lead to increased translational and anterolateral rotational instability of the ACL-deficient knee

Mitautor: C. Fink, Gelenkspunkt

Abstract

Purpose The aim of this biomechanical cadaver study was to evaluate the effects of high-grade posterolateral tibia plateau fractures on the kinematics of anterior cruciate ligament (ACL)-deficient joints; it was hypothesized that, owing to the loss of the integrity of the osseous support of the posterior horn of the lateral meniscus (PHLM), these fractures would influence the biomechanical function of the lateral meniscus (LM) and consequently lead to an increase in anterior translational and anterolateral rotational (ALR) instability.

Methods Eight fresh-frozen cadaveric knees were tested using a six-degree-of-freedom robotic setup (KR 125, KUKA Robotics, Germany) with an attached optical tracking system (Optotrack Certus Motion Capture, Northern Digital, Canada). After the passive path from 0 to 90° was established, a simulated Lachman test and pivot-shift test as well as external rotation (ER) and internal rotation (IR) were applied at 0°, 30°, 60° and 90° of flexion under constant 200 N axial loading. All of the parameters were initially tested in the intact and ACL-deficient states, followed by two different types of posterolateral impression fractures. The dislocation height was 10 mm, and the width was 15 mm in both groups. The intraarticular depth of the fracture corresponded to half of the width of the posterior horn of the lateral meniscus in the first group (Bankart 1) and 100% of the meniscus width in the second group (Bankart 2).

Results There was a significant decrease in knee stability after both types of posterolateral tibial plateau fractures in the ACL-deficient specimens, with increased anterior translation in the simulated Lachman test at 0° and 30° of knee flexion ($p=0.012$). The same effect was seen with regard to the simulated pivot-shift test and IR of the tibia ($p=0.0002$). In the ER and posterior drawer tests, ACL deficiency and concomitant fractures did not influence knee kinematics (n.s.).

Conclusion This study demonstrates that high-grade impression fractures of the posterolateral aspect of the tibial plateau increase the instability of ACL-deficient knees and result in an increase in translational and anterolateral rotational instability.

Milinkovicet al. (2023) The “Bankart knee”: high-grade impression fractures of the posterolateral tibial plateau lead to increased translational and anterolateral rotational instability of the ACL-deficient knee

8 Kadaverknie, 4 male, 4 female, 77.5y

Laxitätsmessungen:
- anterior-posterior Translation
- interne Rotation

Für
- intaktes Knie
- Knie ohne Kreuzband
- 2 medizinische Konditionen (Bankart Knie)

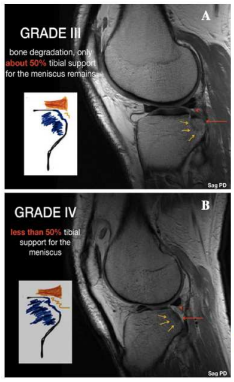

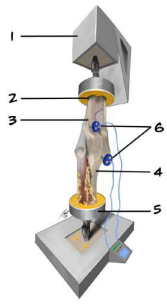

Fig. 2 Biomechanical setup with fixed left cadaveric knee, with: (1) movable component- the robotic arm; (2) aluminium tube; (3) tibia fixed in an upside-down orientation; (4) femur fixed in an upside-down orientation; (5) static component of the robot; (6) two optical sensors fixed to the shaft of tibia and femur with custom-made pins

Milinkovicet al. (2023) The “Bankart knee”: high-grade impression fractures of the posterolateral tibial plateau lead to increased translational and anterolateral rotational instability of the ACL-deficient knee

Anterior-Posterior Translation im gesunden Knie ist ca. 5 mm (89 N)
Ohne Kreuzband doppelt so groß
Bei Bankart Knie noch größer

Fig. 4 Anterior translation of the tibia in Intact, ACL-deficient, Bankart 1 and 2 States at 0–90° of knee flexion. Statistically significant differences compared to the previous states are indicated (*$p < 0.05$, **$p < 0.01$, ***$p < 0.001$). Error bars indicate the standard deviation

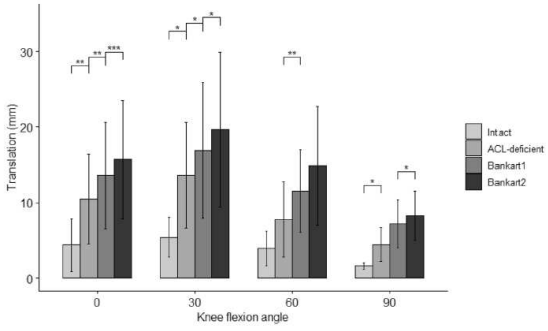

Milinkovicet al. (2023) The “Bankart knee”: high-grade impression fractures of the posterolateral tibial plateau lead to increased translational and anterolateral rotational instability of the ACL-deficient knee

Interne Rotation im gesunden Knie ist ca. 12.5° (4 Nm)
Ohne Kreuzband 14.5°
Bei Bankart Knie noch größer

Fig. 5 Internal rotation of the tibia during a 4 Nm internal rotational torque in Intact, ACL-deficient, Bankart 1 and 2 states in 0°–90° of knee flexion. Statistically significant differences compared to the previous states are indicated (*$p<0.05$, **$p<0.01$, ***$p<0.001$). Error bars indicate the standard deviation

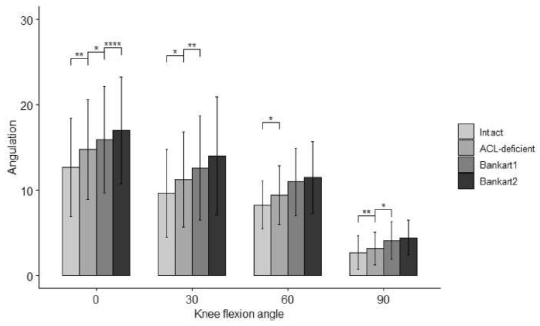

Milinkovicet al. (2023) The “Bankart knee”: high-grade impression fractures of the posterolateral tibial plateau lead to increased translational and anterolateral rotational instability of the ACL-deficient knee

Schlussfolgerung

Das Knie hat nur eine begrenzte Stabilität
Ohne vorderes Kreuzband ist diese bereits deutlich reduziert

Bei einem Bankart Knie (Verletzung) noch mehr.